Hanle-effect studies on the $(5p^4 6s)\,^4P_{5/2}$ state of iodine

Lloyd G. Williams and David R. Crosley
Department of Chemistry, University of Wisconsin, Madison, Wisconsin 53706
(Received 13 September 1973)

Hanle-effect measurements have been made on the $(5p^4 6s)\,^4P_{5/2}$ state of iodine, which is connected to the ground state via the 1830-Å line. The atomic iodine is produced by thermal dissociation of I_2, and is excited by unpolarized resonance radiation. Using the value of g_J obtained by Keiss and Corliss from high-field Zeeman splittings, we find a radiative lifetime of 57.9 ± 1.4 nsec (all errors quoted are 67% confidence limits). Neither coherence narrowing nor self-broadening is observed, and we place an upper limit of 200 Å^2 on the latter process. Cross sections for broadening of the Hanle effect by the rare gases are found to be (in Å^2): He: 9.8 ± 1.1; Ne: 19.5 ± 1.6; Ar: 37.6 ± 3.1; Kr: 38.7 ± 3.8; Xe: 49.2 ± 3.1. The relative values of these cross sections are seen to be in agreement with the predictions of a van der Waals interaction.

I. INTRODUCTION

Lifetimes and collision cross sections are important parameters characterizing the excited states of atoms and molecules. The Hanle effect,[1] or zero-field level-crossing technique, permits an accurate measurement of both of these quantities. The Hanle effect depends on the coherence which is established in the excited state when a set of Zeeman sublevels is degenerate to within a natural linewidth. Application of an external (magnetic) field removes the degeneracy and destroys the coherence; this is manifested as a field-dependent change in the angular distribution of the fluorescence. We use here a right-angle geometry and unpolarized light, thus detecting crossings between levels having $\Delta m = \pm 2$ (the upper-state population distribution so created is termed "alignment"). The fluorescence $\mathcal{J}$ has a Lorentzian dependence on the magnetic field H:

$$\mathcal{J} \propto 1 - \frac{\mathcal{P}}{1 + (2g\mu_B H\tau/\hbar)^2}\,, \tag{1}$$

where g is the Landé g factor for the level involved, τ is the effective lifetime for the coherence, μ_B is the Bohr magneton and $\hbar$ is Planck's constant divided by 2π. $\mathcal{P}$ represents the fraction of fluorescence dependent on field and may be calculated using knowledge of the angular momenta of the states involved, the polarizations, and the line shapes of the exciting and absorbed radiation.

In general, there are a number of contributions to τ. Important in this investigation are only the radiative lifetime τ_r and the destruction of coherence by collisions between the excited state and foreign atoms:

$$1/\tau = 1/\tau_r + n\bar{v}\sigma\,. \tag{2}$$

Here, n is the density of foreign gas atoms, $\bar{v}$ is the mean relative velocity of the iodine and perturbing atom, and σ is the cross section for destruction of coherence ("collisional broadening"). The measured Hanle-effect width at zero foreign-gas pressure yields τ_r, while the slope of the width vs n yields the cross section σ.

We here report the extension of Hanle-effect studies to a group-VII atom, in an investigation of the radiative lifetime and broadening cross sections (with rare gases) of the $(5p^4 6s)\,^4P_{5/2}$ state of iodine. A number of the states arising from this configuration are shown in Fig. 1. The 1830-Å resonance line connects the $^4P_{5/2}$ state with the ground $(5p^5)\,^2P_{3/2}$ state; the relatively strong character of this quartet-doublet transition is accounted for by mixing of the $^2D_{5/2}$ state with the $^4P_{5/2}$ state.

The lifetime of this state is of interest for a number of reasons. From it may be obtained oscillator strengths for use in absorption measurements, which are becoming of increasing utility in monitoring ground-state iodine concentrations in chemical kinetics. We compare our Hanle-effect result with lifetimes calculated from absorption coefficients, measured by ourselves and by others.[2,3] We conclude that, due to the complex hyperfine structure of the 1830-Å line, such concentration measurements can be in error unless lamp and absorption-line profiles match well. The oscillator strengths may also be used to assess the validity of excited-state wave functions and to calculate lifetimes of other states of the same configuration (provided the extent of spin-orbit splitting is known). Knowledge of τ_r is also necessary for interpretation of the collisional broadening, as well as for studies on energy transfer involving the excited state. A previous determination of τ_r

has been made by Lawrence[4] using a phase-shift technique; his experimental result had a large uncertainty due to uncertainty in the correction for cascading transitions into the $^4P_{5/2}$ state. He also calculated τ_r using the (more accurate) measurement of the lifetime of the $(5p^4 6s)\ ^2P_{3/2}$ state (see Fig. 1) and an intermediate angular-momentum coupling scheme. Lawrence's measurement is in disagreement with our Hanle-effect results but his calculated τ_r compares quite well.

A number of investigators[5-9] have calculated cross sections for the collisional broadening, by rare gases, of the Hanle effect in several atoms (though not iodine). These calculations assume a van der Waals interaction and straight-line trajectory; such a mechanism leads to a predicted ratio $\sigma_{He}/\sigma_{Ne} \sim 0.6$. Previous experimental results yielding a ratio of $\sigma_{He}/\sigma_{Ne} \sim 1$ have been explained[8] as due to an enhancement of σ_{He} due to strong collisions. We find a ratio of 0.5 for the broadening in iodine, suggesting that strong collisions are not so important here.

II. EXPERIMENTAL DETAILS AND RESULTS

A. Measurements on pure iodine

The basic apparatus used for the Hanle-effect measurements (see Fig. 2) is typical for such experiments. A T-shaped quartz cell, with short-focal-length Suprasil lenses sealed in place of windows, contains the iodine atoms. An 8-mm-diam tube connects the cell to a reservoir in which are placed iodine crystals which have been purified by repeated vacuum distillation. The reservoir is surrounded by a thermostated bath (FTS Systems, Inc. cooling bath with temperature controller, maintaining the temperature to ±0.1°C) operated between -40 and 0°C; this controls the I_2 vapor pressure P_{I_2}. The fluorescence cell is maintained at ~640°C by a heater coil,[10] producing iodine atoms by thermal dissociation. The iodine atom pressure within the cell, P_I, is calculated from the I_2 pressure in the reservoir, the equilibrium constant K_p for $I_2 \rightleftharpoons 2I$ at the temperature of the cell, and an assumption regarding flow conditions between the reservoir and the cell. Using the criteria given by Dushman,[11] we find that over our usual operating ranges (below 10 mTorr pressure) the flow may be characterized as effusive; i.e., the total number density must be the same throughout all regions of the system. Under these conditions P_I is given by

$$P_I = \frac{K_P}{2}\left\{\left[\frac{1}{2} + \frac{4}{K_P}\left(\frac{T_c}{T_R}\right)^{1/2} P_{I_2}\right]^{1/2} - \frac{1}{\sqrt{2}}\right\}, \qquad (3)$$

where T_c and T_R are the cell and reservoir temperatures. P_{I_2} and K_P are calculated using thermodynamic data.[12] T_c is measured by a thermocouple in contact with the cell near the center. (Measurements on other similar cells with three thermocouples show that the temperature may be 40–50° cooler at the windows. The uncertainty thus introduced into P_I is $\lesssim 2\%$ and produces a negligible

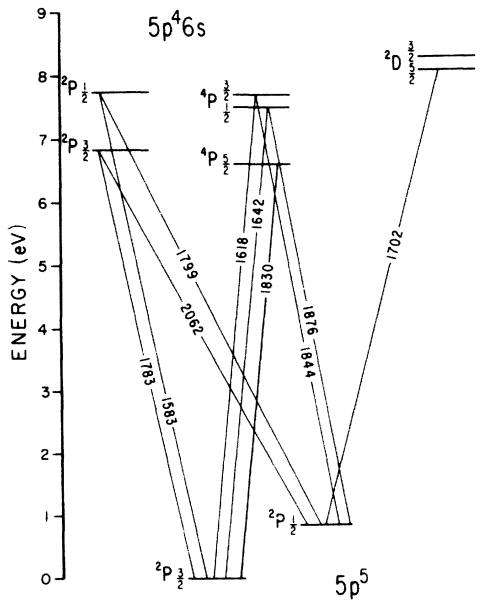

FIG. 1. Some states of iodine arising from the $5p^5$ and the $5p^4 6s$ configurations, and the spectral lines connecting them.

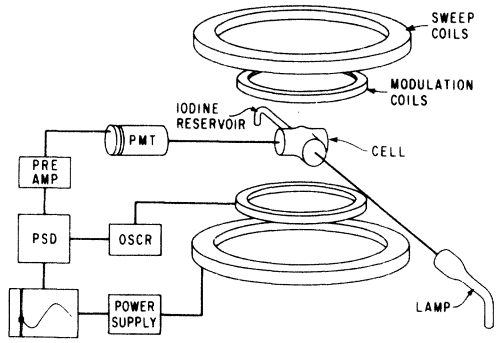

FIG. 2. Experimental apparatus used for the Hanle-effect measurements. The photomultiplier (PMT) signal, amplified by the preamplifier, is fed into the phase-sensitive detector (PSD), whose reference channel is driven by an audio oscillator (OSCR) which also drives the modulation coils. The y axis of the recorder follows the PSD output while the x axis is driven by the voltage across a small resistance in series with the sweep coils. Not shown are lenses or the nitrogen flushing tubes between the lamp and cell, and the cell and PMT. Also not shown are the bucking coils, the thermostated cooling bath surrounding the I_2 reservior, or the attached vacuum line.

error in our results.)

The resonance fluorescence is excited by an electrodeless discharge lamp containing iodine vapor and ~0.5-Torr argon. By maintaining the I_2 pressure at ~30 mTorr using an ice bath, it is possible to obtain a lamp with an ultraviolet output which is predominantly 1830-Å radiation. The fluorescence from the cell is detected by a solar blind photomultiplier (EMI G26EA215) with a response which falls sharply at wavelengths longer than 1900 Å. The optical paths between the lamp and cell, and between the cell and the photomultiplier, are flushed with dry nitrogen to eliminate absorption of the 1830-Å line by the oxygen in the air. The absorption at shorter wavelengths due to the nitrogen ensures no contribution from radiation with $\lambda < 1700$ Å, and, under our operating conditions, the lamp output at 1783 Å is $< \frac{1}{7}$ of that at 1830 Å. This ensures that the 1830-Å line is the predominant feature in the observed fluorescence. This has been verified by observation of the overall fluorescence and the Hanle-effect signal using a small (Heath EU700) monochromator, set at 1830 Å with a ~30-Å bandpass and flushed with N_2, to disperse the fluorescence. The cell is situated at the center of five pairs of Helmholtz coils. One of these provides a field sweep between −6 and +6 G, a second is used to apply a 260 Hz modulation field of amplitude ~1.5 G, and three orthogonal sets are used to cancel the earth's field to within ±5 mG in the cell region.

The directions of propagation of the (unpolarized) exciting and fluorescent light and the static field are all mutually perpendicular. With this geometry, the Hanle-effect signal has an inverted Lorentzian dependence on the field strength. The $^4P_{5/2}$ state has five different hyperfine levels which can exhibit a Hanle effect. However, because $I = J = \frac{5}{2}$ for this state, all the hyperfine levels have the same g value. Thus the Hanle-effect signal appears as a single Lorentzian rather than a composite of several Lorentzians with different widths. Use of the modulation field and phase-sensitive detector (Ithaco 391) improves the signal-to-noise ratio considerably. The output of the phase-sensitive detector closely resembles the derivative dg/dH from Eq. (1). The resulting curve is fitted, using a nonlinear least-squares routine, to a formula given by Wahlquist[13] for the first Fourier component of a modulation-broadened Lorentzian.[14] The amplitude of the modulation field, necessary for the fitting procedure, was measured for each series of runs. The results for a typical run are shown in Fig. 3.

Hanle-effect measurements were made as a function of iodine-atom number density n_I, where n_I was calculated using Eq. (3). Shown in Fig. 4 are the fitted full widths at half-maximum (FWHM) of the Hanle-effect signal as a function of n_I. The error bars represent 1-σ confidence levels[15] calculated from the line-fitting program.

In general, the width of the Hanle effect in the absence of any foreign gas depends on pressure through two effects: coherence narrowing and self-broadening. We feel that the data exhibited in Fig. 4 show evidence of neither of these effects, to within experimental error (see Sec. III). Accordingly, we average the data shown to obtain a FWHM of 2.49 ± 0.12 G. This uncertainty (2-σ level) is calculated considering as uncorrelated sources of error (i) the line-fit confidence limits (± 0.04 G); (ii) the uncertainty in the magnetic-field calibration (1.5%), which was made using a Bell Hall-ef-

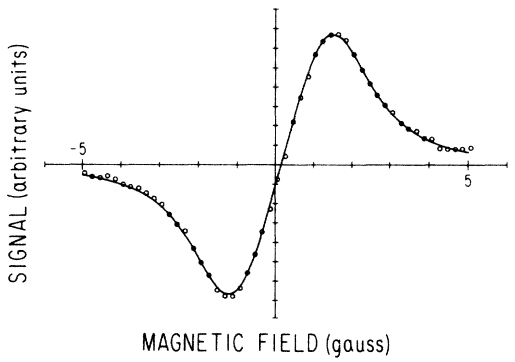

FIG. 3. Hanle-effect run, here shown for pure iodine at 5×10^{13} cm^{-3}. The circles are the experimental points and the line represents the computer fit. The signal is offset from zero field owing to time constant effects (accounted for in the fitting procedure); the time constant was 12.5 sec and the entire run took about 40 min.

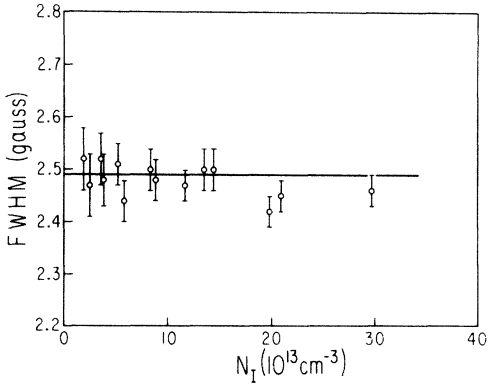

FIG. 4. Hanle-effect results (full width at half-maximum of the Lorentzian) as a function of iodine-atom number density. The error bars shown represent the line-fit confidence limits; the horizontal line at 2.49 G is at the average of all the runs made (some points represent more than one run at that number density).

fect Gaussmeter (in turn calibrated at one point using a fixed-frequency ESR spectrometer); (iii) chart linearity (estimated at 1%); and (iv) the contribution from uncertainty in the modulation-field measurement (estimated by calculation as 0.03 G).

The radiative lifetime may now be extracted from Eq. (1); use of this relationship requires knowledge of the g value of the $^4P_{5/2}$ state. We take $g_J = 1.576$ from the high-field Zeeman-splitting measurements of Keiss and Corliss.[16] Because $I = J$ for this state, $g_F = \frac{1}{2} g_J$ for all the levels of any total angular momentum F. This results in a radiative lifetime of 57.9 ± 2.8 nsec.

From the width measured at the highest value of n_I ($\sim 3 \times 10^{14}$ cm^{-3}) and this value for τ_r we may place an upper limit of 200 Å^2 on the self-broadening cross section.

B. Broadening due to rare gases

The Hanle-effect signal can also be broadened by collisions with foreign gases, which reduce the apparent lifetime of the level according to Eq. (2). A vacuum line was attached to the cell for filling with rare gases while leaving it positioned in the Hanle-effect setup.

Pressures of the rare gases were measured with an NRC Alphatron gauge. The Alphatron was in turn calibrated against a McLeod gauge after all the Hanle-effect measurements were made (in order to avoid contamination of the cell with mercury). The McLeod gauge (a CVC model GM-100A) was used on the 1–10-Torr scale with a few points in the 0.1–1-Torr range, so that the systematic errors often associated with McLeod gauge operation[17] should be negligible. The calibration factors were taken from least-squares fits of Alphatron readings vs McLeod gauge readings over a pressure range of at least several Torr. The consistency of these fits is better than the readability of the Alphatron. The results of the calibration runs[18] are listed in Table I.

TABLE I. Calibration data for Alphatron gauge used for the rare-gas pressure measurements.

Gas	Absolute sensitivity[a]	Sensitivity relative to air	
		Present calibration[b]	Old NRC manual[c]
Air	0.84 ± 0.04	...	...
He	3.34 ± 0.06	3.97 ± 0.22	4.74
Ne	1.41 ± 0.02	1.67 ± 0.09	1.56
Ar	0.692 ± 0.006	0.822 ± 0.043	0.84
Kr	0.440 ± 0.005	0.522 ± 0.027	...
Xe	0.286 ± 0.003	0.340 ± 0.018	0.33

[a] Actual pressure divided by measured pressure.
[b] Note that nearly all the uncertainty here comes from the less carefully measured air calibration.
[c] See Ref. 18.

The measured rare-gas pressure is, effectively, that measured in the room-temperature portion of the cell. Here we are dealing with high enough pressures that the hydrodynamic limit[11] holds for the gas flow between the different regions of the cell, and the rare-gas number densities are calculated under this assumption of equal pressure throughout the system. A calculation of the rate of diffusion of He through the walls of the hot cell was made using the formulation due to Dushman[11] and the data of Norton.[19] The result is a pressure decrease of $\lesssim 1\%$ per hour; since the He runs are made within 1–2 h after the filling and pressure measurement, we neglect effects of any such diffusion. The reservoir was kept at −30°C for these runs, corresponding to $n_1 \sim 3 \times 10^{13}$ cm^{-3}, which was the value yielding the optimum signal-to-noise ratio.

In Fig. 5 are displayed the FWHM results as a function of rare-gas pressure. The lines are least-squares fits with each point weighted by the inverse of the error bars. The fitted slopes and intercepts, together with their calculated standard deviations, are given in Table II.

From the slopes and τ_r, we can calculate the collision-broadening cross sections σ. $\bar{v}$ is calculated using a cell temperature of 913 °K. The uncertainty

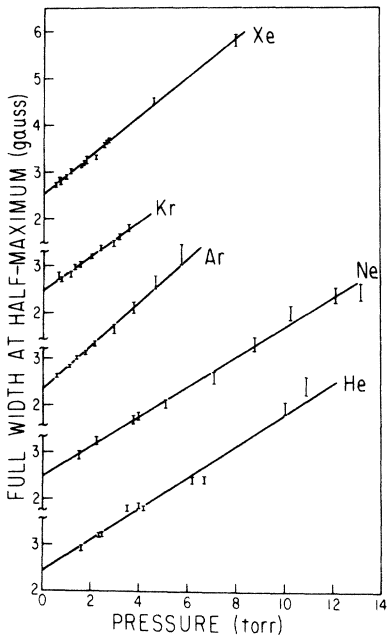

FIG. 5. Hanle-effect results (FWHM) as a function of rare-gas pressure. The bars represent the 1-σ limits of uncertainty from the line fits, and the lines drawn are the least-squares fits (see text).

in σ comes from several sources, which are combined as uncorrelated: (a) the uncertainty in the slope determinations; (b) the uncertainty in the values of n for each gas (this is based on uncertainties in reading and calibrating the Alphatron but does not take into account any assessment of uncertainty in the hydrodynamic limit assumption); and (c) the uncertainty ΔT_c in the cell temperature. ΔT_c is estimated at ±50°C, owing to possible variation of the temperature over the cell and lack of knowledge of precisely what region the thermocouple is sampling. We note, however, that this contribution to the total uncertainty (±3%) is relevant to absolute cross sections. Since results with different gases come from measurements at the same temperature, this source of error will be much less in influencing *relative* sizes of the broadening cross sections. The results for σ and the (1-σ level) estimate of uncertainties are also listed in Table II.

C. Absorption measurements

In an effort to reconcile our Hanle-effect results with previously reported absorption coefficients, we undertook a measurement of 1830-Å line absorption as a function of iodine-atom density. An absorption cell of 5-cm length was constructed in the manner of the fluorescence cell except that windows, not lenses, were used. Iodine atomic-line radiation from the electrodeless discharge lamp passed through the absorption cell and was focused on the slit of the Heath monochromator, set at 1830 Å. n_I was calculated as described above. The measured absorption was reduced to an absorption coefficient in the fashion described by Mitchell and Zemansky.[20] The analysis was made using the (greatly oversimplified) assumption of a single Doppler-broadened line; hyperfine structure was accounted for by means of a simple correction factor, as suggested by Tellinghuisen.[3(a)]

The observed value of the absorption coefficient was exceedingly sensitive to the temperature of the cell, varying a factor of 100 between 300 and 700°C, and was always lower than that calculated using the Hanle-effect value of τ_r. Certainly some such variation is not unexpected. The lamp has a temperature probably close to that of its walls, measured to be 130°C, and the hyperfine structure of the 1830-Å line is quite complex (see Fig. 6), so that the overlap will change considerably with cell temperature.[21] Tellinghuisen[3(a)] has also found a strong temperature dependence of the absorption coefficients for both the 1783- and 1830-Å lines. In both studies, the correspondence with our Hanle-effect lifetime is closest for the lowest cell temperature employed, but still yields an absorption coefficient too small by a factor of 1.5–2. It would appear that the hyperfine structure greatly complicates the relationship between the absorption coefficient and n_I, for differing cell and lamp temperatures.

Producing iodine atoms from the stoichiometric reaction $Cl + ICl \rightarrow Cl_2 + I$, and using known amounts of ICl to determine n_I, Clyne and Cruse[2] have also measured the 1830-Å line absorption. Their results, shown in their Fig. 4, can be reduced[22] to a lifetime of 66 nsec, comparing much better with our Hanle-effect value. Clyne and Cruse use ~1 Torr of argon carrier gas in both their lamp and absorption flow tube, so that the emission and absorption lines likely have the same profile. This good correspondence is encouraging in view of the fact that kinetic measurements where n_I is monitored using absorption techniques are often carried out in the excess of other gases.

Using our measured absorption coefficients for the operating conditions of the fluorescence cell, we have calculated the fluorescence signal as a function of n_I, taking into account the reabsorption of fluorescence, and the fact that the photomulti-

TABLE II. Results of the rare-gas collision-broadening experiments. The uncertainties given for the slopes and intercepts are taken from the uncertainties in the fits shown in Fig. 5, while the uncertainties in the cross sections include as well contributions from the temperature and pressure measurements.

Gas	Slope (G Torr^{-1})	Intercept (G)	σ(Å^2)
He	0.334±0.015	2.43±0.06	9.8±1.1
Ne	0.313±0.009	2.51±0.04	19.5±1.6
Ar	0.458±0.015	2.36±0.02	37.6±3.1
Kr	0.365±0.015	2.48±0.02	38.7±3.8
Xe	0.411±0.007	2.53±0.01	49.7±3.1

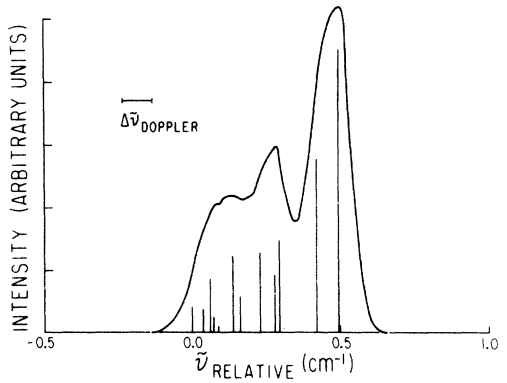

FIG. 6. Calculated structure of the 1830-Å absorption line. The vertical lines show the relative contributions from different hyperfine components. The curve is the sum of the Doppler-broadened lines, calculated for a temperature of 640°C corresponding to the usual T_c.

plier views only the center of the cell. A comparison of this calculation with measured total fluorescence signal, and the fitted Hanle-effect amplitudes, as a function of n_I, shows agreement to within experimental error except at the highest n_I used. This suggests that the effective absorption coefficient under the usual operating conditions during the Hanle-effect measurements is significantly smaller than would be predicted by τ_r.

D. Polarization measurements and calculations

The Hanle-effect amplitude relative to the field-independent part of the signal is denoted by $\mathcal{P}$ in Eq. (1). This was measured using both the total fluorescent light falling on the photomultiplier as well as the resultant signal after dispersion through the Heath monochromator. The signal-to-noise ratio was low in both cases (most of our noise in all the experiments comes from lamp fluctuations) and yielded a value for $\mathcal{P}$ of $2 \pm 1\%$.

A theoretical prediction of $\mathcal{P}$ depends on assumptions regarding the lamp line shape relative to the absorption line shape. We have carried out a calculation of $\mathcal{P}$ (see Appendix) using three approximations: (a) "white light," i.e., uniform lamp intensity as a function of wavelength; (b) "isolated lines," i.e., a lamp intensity for a given $F \rightarrow F'$ component (F and F' are the ground- and excited-state total angular-momentum quantum numbers) given by the theoretical line strengths; (c) "overlapping lines," i.e., a lamp intensity for each $F \rightarrow F'$ component given by the intensity curve of Fig. 6 for the wavelength corresponding to the center of that component.

The results of the calculation yield the following for $\mathcal{P}$: white light, 2.9%; isolated lines, 4.7%; and overlapping lines, 3.8%. (It is noteworthy that the high value of nuclear spin I reduces the over-all $\mathcal{P}$ from a value for $I = 0$ in a $J = \frac{3}{2} \rightarrow \frac{5}{2} \rightarrow \frac{3}{2}$ sequence of 37% to these much smaller amounts.) In view of the poor accuracy of the experimental data, this criterion does not provide knowledge of the lamp line shape. Self-reversal in the stronger components with high values of F and F', as well as I_2 absorption in the lamp, may be responsible for the lower experimental value of $\mathcal{P}$.

III. DISCUSSION

A. Radiative lifetime results

Our result for the radiative lifetime of the $(5p^4 6s)\,^4P_{5/2}$ state, 57.9 ± 1.4 nsec, is in agreement only at the limit of uncertainty with the previously determined phase-shift value[4] of 80 ± 30 nsec. The large uncertainty there was due to the necessity of correcting the measured result for cascading into the $^4P_{5/2}$ state (the excited iodine was produced by electron bombardment of IF_5). This points up the complementary nature of these techniques: Hanle-effect measurements are generally freer from systematic errors compared to phase-shift studies, but cannot be carried out so readily over a large number of levels.

Lawrence[4] also calculated a lifetime for the $^4P_{5/2}$ state based on an intermediate-coupling scheme. The radial factor in the matrix element is scaled to his measurement of the lifetime of the $^2P_{3/2}$ state arising from the same configuration (1783-Å line), which does not suffer from cascade problems. The coupling scheme is determined by an over-all fit of the spin-orbit parameter ζ to the energy differences of the several states arising from the $5p^4 6s$ configuration. Lawrence's calculated result for τ_r ($^4P_{5/2}$) is 63 ± 11 nsec (since $\tau_r \propto \zeta^{-2}$, his fit of the term splittings to $\sim \pm 8\%$ implies an uncertainty in the calculated τ_r of $\sim \pm 16\%$), in much better agreement with our measurement. This is not surprising, since his τ_r ($^2P_{3/2}$) is more precise (quoted as $\pm 20\%$ or better).[23]

B. Absence of coherence narrowing and resonant self-broadening

We have interpreted the data shown in Fig. 4 as exhibiting neither coherence narrowing nor self-broadening, although the measurements are carried out to an iodine number density of 3×10^{14} cm^{-3}.

Coherence narrowing results from radiative trapping of photons maintaining coherent excitation in a sequence of absorption/emission events, leading to an apparent lengthening of the coherence lifetime and narrowing of the Hanle-effect signal. Its magnitude at a given number density is governed by two effects, the probability of reabsorption of a photon within the fluorescence cell, and a factor α dependent on the angular momentum of the states involved. For the oscillator strength $f = 0.013$ corresponding to $\tau_r = 58$ nsec, the cell should be optically thick at $n_I = 3 \times 10^{14}$ cm^{-3}. However, our absorption measurements (see above) indicate that, for our typical $T_c = 640$°C, we have a significantly lower effective absorption coefficient ($k_0/N \approx 1 \times 10^{-15}$ cm^2) than implied by τ_r, and consequently a low probability of reabsorption. The factor α for a $J = \frac{5}{2} \rightarrow J = \frac{3}{2}$ transition in the absence of nuclear spin is given in Saloman and Happer[24] as 0.196; this reflects the maximum portion which the apparent lifetime may be lengthened for transitions involving these high values of J. The presence of nuclear spin reduces α significantly more, as may be seen from Barrat's studies[25] on coherence narrowing in Hg. Thus our experimental upper limit of 2% for the coherence narrowing at $n_I = 3 \times 10^{14}$ cm^{-3} is in

agreement with expectations.

Resonant self-broadening of the Hanle effect occurs by a dipole-type interaction between a ground-state and an excited-state iodine atom, and is proportional to $|\langle g|\vec{r}|e\rangle|^2$ which may in turn be evaluated in terms of λ (the wavelength of the transition) and τ_r. For a $J=1\rightarrow 0$ transition in the absence of nuclear spin, this leads to a predicted self-broadening cross section[5]

$$\sigma = \frac{1}{10\pi}\frac{\lambda^3}{\tau_r \bar{v}} . \tag{4}$$

For higher values of J, and nonzero nuclear spin, one expects a smaller cross section than given by Eq. (4). This is in agreement with the fact that our experimental upper limit for σ of 200 Å^2 is smaller than the 800 Å^2 predicted by Eq. (4) for $\lambda = 1830$ Å and $\tau_r = 58$ nsec.

C. Rare-gas collision-broadening cross sections

Theoretical predictions for collision-broadening cross sections have been made by a number of investigators.[5-9] Because the cross sections for Hanle-effect broadening are large, it is reasonable to begin with the supposition that the dominant interaction is due to the long-range dipole-dipole forces (van der Waals forces):

$$V(\vec{R}) = \frac{\vec{p}_I\cdot\vec{p}_g - 3(\vec{p}_I\cdot\hat{\vec{R}})(\vec{p}_g\cdot\hat{\vec{R}})}{R^3} .$$

Here, $\vec{p}_I$ and $\vec{p}_g$ are the dipole-moment operators for the iodine and the colliding rare-gas, respectively; $\vec{R}$ is the separation between the atoms. Using a perturbation treatment and integrating V over a straight-line trajectory, one can write

$$\sigma = C\left(\frac{\langle p_I^2\rangle\langle p_g^2\rangle}{\Delta E}\right)^{2/5}\frac{\langle v^{3/5}\rangle}{\langle v\rangle} , \tag{5}$$

where C is a numerical constant depending on the angular momenta of the states involved. $\langle p_I^2\rangle$ is evaluated for the $(5p^46s)\,^4P_{5/2}$ state and $\langle p_g^2\rangle$ for the ground state of the colliding rare gas. The closure approximation has been invoked, so that ΔE is the energy difference between "an average" excited state of each atom and the state for which $\langle p^2\rangle$ is calculated. The velocity averages are taken over a Maxwellian distribution, for which it can be shown that

$$\langle v^{3/5}\rangle/\langle v\rangle = 0.931(\tfrac{1}{2}\pi^{1/2}\langle v\rangle)^{2/5} \propto (1/\mu)^{1/5} ,$$

where μ is the reduced mass of the colliding pair. Thus for a particular rare gas i,

$$\sigma_i = k(\langle p_i^2\rangle/\Delta E)^{2/5}(1/\mu)^{1/5} , \tag{6}$$

where k is a constant independent of the rare gas.

The quantity in brackets in Eq. (6) is essentially the C_6 coefficient for a collision between an excited iodine atom and a rare gas. From London's original derivation of the dispersion energy,[26] one can write for two colliding atoms A and B the approximation

$$C_6 = \frac{3}{2}\frac{W_A W_B}{W_A + W_B}\alpha_A\alpha_B ,$$

where W is the ionization potential and α the polarizability. Again, removing the terms independent of the rare gas, we rewrite Eq. (6) as

$$\sigma_i = k'\left(\frac{W_e W_i}{W_e + W_i}\alpha_i\right)^{2/5}\left(\frac{1}{\mu}\right)^{1/5} \equiv k' x_i , \tag{7}$$

where e refers to the excited iodine atom. We use for W_e the ionization potential[27] of ground-state iodine minus the energy difference between the ground state and the $^4P_{5/2}$ state, or 3.67 eV. The ionization potentials for the rare gases[27] are listed in Table III. The values of the polarizabilities of the rare gases, also listed in Table III, are taken from index of refraction measurements.[28]

TABLE III. Data for the rare gases used in the calculation of the relative cross sections for collision broadening.

Gas	Ionization potential (eV)	α (Å^3)	x
He	24.580	0.2051	0.295
Ne	21.559	0.395	0.514
Ar	15.755	1.64	1.000
Kr	13.996	2.48	1.284
Xe	12.127	4.04	1.620

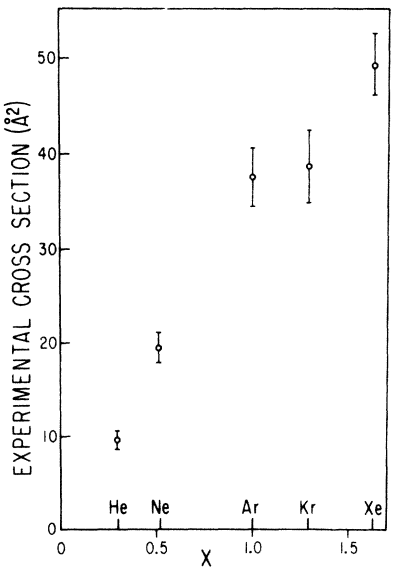

FIG. 7. Collision-broadening cross sections for the rare gases vs the parameter x, calculated as described in the text.

Using these data, we calculate the values of x_i for each of the rare gases. The observed cross sections $(\sigma_i)_{obs}$ are plotted vs x_i in Fig. 7.

The relative values of the cross sections follow quite well the predictions using the van der Waals mechanism. In particular, we draw attention to the observed ratio $\sigma_{He}/\sigma_{He} = 0.50 \pm 0.07$, compared to the predicted ratio of 0.576.

Cross sections have been measured for the broadening of the Hanle effect[29] and double-resonance signal[30] in the $(6s6p)\,^3P_1$ state of Hg and of the Hanle effect in eight levels of the $2p^5 3p$ configuration of Ne,[31] and for the equivalent depolarization of fluorescence in the $^3P_1$ state of Hg[32] and the $(6s^2 6p^2)\,^3P_1$ and $^3P_2$ states of Pb.[9] All of these results show a ratio $\sigma_{He}/\sigma_{Ne} \sim 1$, in contrast to a value of 0.57–0.63 predicted for all of these systems by Eq. (7).[33] The relative values of the predicted cross sections for these systems with Ar, Kr, and Xe compared to Ne are in reasonable accord with experiment. It has been suggested[8] that the anomalously high value for σ_{He} compared to cross sections for the other rare gases is due to the importance of shorter-range forces in collisions with He, which has such a low polarizability.

For the $(6s^2 6p\,7s)\,^3P_1^0$ state of Pb, Gibbs[9] has determined $\sigma_{He}/\sigma_{Ne} = 0.61 \pm 0.17$, also in agreement with the prediction from van der Waals broadening. In both the case of iodine and this state of lead, the excited electron is in an s state of higher principal quantum number than the outer electrons of the ground-state configuration, compared to the excited configurations in Hg and the other states of Pb, where the electrons remain in the $n = 6$ shell. One might anticipate a higher polarizability for the excited states of I and the $^3P_1^0$ state of Pb, such that longer-range interactions would dominate even in the case of He. We note, however, that if this were the only consideration, one would expect the σ_{He}/σ_{Ne} ratio for broadening of the $2p^5 3p$ neon levels to decrease with increasing polarizability of the individual levels. There appears to be no correlation between the measured ratio[8] and the calculated polarizabilities[31] of these levels.[34]

A calculation of the absolute cross sections is hampered by the lack of a reliable value for $\langle p_I^2 \rangle$ for the $^4P_{5/2}$ state, as well as the necessity to correct for the effects of hyperfine structure, which will reduce the cross sections from the values calculated presuming $I = 0$. The use of Slater wave functions[35] for the $6s$ orbital of iodine predicts $\langle r^2 \rangle_{6s} \sim 120 a_0^2$, which is unrealistically large, and a cross section for broadening by helium of $\sim 20C$ (in units of Å^2), where C is the angular momentum factor in Eq. (5). Since C is of the order of 1, and in view of the value used for $\langle r^2 \rangle_{6s}$, the absolute predicted values are at least in the proper range.

Ground-state iodine atoms can also broaden the Hanle effect through a nonresonant second-order van der Waals mechanism, acting in essence like a rare-gas atom. Using Slater orbital values for $5p^5$ iodine (where they are expected to be a more reasonable approximation), we calculate a nonresonant self-broadening cross section $\sigma_{NR} \sim 10\sigma_{He}$. Comparison of this with the experimental value for σ_{He} (to avoid complications due to the value of value of C) predicts $\sigma_{NR} \sim 100$ Å, less than our experimental upper limit on the total[36] (resonant plus nonresonant) self-broadening cross section.

ACKNOWLEDGMENTS

We gratefully acknowledge support from the National Science Foundation, under Grant No. GP-17790, and from the Wisconsin Alumni Research Foundation.

APPENDIX

A starting point for the calculation is the Breit formula[37] for the steady-state rate $R_{\alpha f}$ of emission of photons of polarization $\vec{f}$, after excitation by photons of polarization $\vec{a}$:

$$R_{\alpha f} = \sum_{\mu\mu'} \frac{\mathfrak{A}_{\mu\mu'}(\vec{a})\mathfrak{F}_{\mu'\mu}(\vec{f})}{1 + (\Delta E_{\mu'\mu}\tau/\hbar)^2} ,$$

where μ and μ' label the excited-state wave functions; $\Delta E_{\mu\mu'}$ is their energy difference. $\mathfrak{A}_{\mu\mu'}(\vec{a})$ is given by

$$\mathfrak{A}_{\mu\mu'}(\vec{a}) = \sum_m \langle \mu | \vec{a}\cdot\vec{r} | m \rangle \langle m | \vec{a}\cdot\vec{r} | \mu' \rangle ,$$

where m refers to the ground state and r is the dipole-moment operator; $\mathfrak{F}_{\mu'\mu}(\vec{f})$ has the same form.

Since the $^4P_{5/2} \rightarrow {}^2P_{3/2}$ line is nominally forbidden and arises through $^2D_{5/2}$ mixing, the calculation is performed simply for a $J = \frac{5}{2} \rightarrow J = \frac{3}{2}$ transition without regard to multiplicity. The levels are described by the quantum numbers F and m_F. A separate rate $R_{\alpha f}$ is calculated for each upper-state hyperfine level F', for all possible initial and terminal ground-state levels F_i and F_t in the sequence $F_i \rightarrow F' \rightarrow F_t$; the over-all $R_{\alpha f}$ is equal to the sum of these. The three approximations to the lamp profile are accounted for by weighting the $\mathfrak{A}_{\mu\mu'}(a)$ matrices for a given $F_i \rightarrow F'$ by the intensity appropriate to that approximation. The matrix elements themselves are calculated using standard vector-coupling formulas given by Condon and Shortley.[38]

The results of the calculation show that the sign

as well as the magnitude of $\mathcal{P}$ varies with upper-state hyperfine level and transition sequence. Because negative as well as positive values of $\mathcal{P}$ occur, the over-all result is quite sensitive to a proper choice of lamp profile.

---

[1]For reviews, see W. Happer, in *Beam Foil Spectroscopy*, edited by S. Bashkin (Gordon and Breach, New York, 1968), p. 305; B. Budick, Adv. At. Mol. Phys. 3, 73 (1967).

[2]M. A. A. Clyne and H. W. Cruse, Trans. Faraday Soc. 67, 2869 (1971).

[3](a) J. B. Tellinghuisen, Ph.D. thesis (University of California, Berkeley) (unpublished), UCRL Report No. UCRL-19112 (1969); (b) L. Brewer and J. B. Tellinghuisen, J. Chem. Phys. 54, 5133 (1971).

[4]G. M. Lawrence, Astrophys. J. 148, 261 (1967).

[5]F. W. Byron and H. M. Foley, Phys. Rev. 134, A625 (1964).

[6]A. Omont, J. Phys. (Paris) 26, 26 (1965); A. Omont and J. Meunier, Phys. Rev. 169, 92 (1968).

[7]C. H. Wang and W. J. Tomlinson, Phys. Rev. 181, 115 (1969).

[8]C. G. Carrington and A. Corney, J. Phys. B 4, 869 (1971).

[9]H. M. Gibbs, Phys. Rev. A 5, 2408 (1972).

[10]The heater coil is wound in a bifilar manner so as not to produce ac fields broadening the Hanle-effect signal. Runs at 4.1 and 3.6 A showed no difference in width.

[11]S. Dushman, *Scientific Foundations of Vacuum Technique* (Wiley, New York, 1949).

[12]*JANAF Thermochemical Tables* (The Dow Chemical Company, Midland, Mich., 1961).

[13]H. Wahlquist, J. Chem. Phys. 35, 1708 (1961).

[14]Inclusion of a dispersion component on some runs (even those which appeared to the eye to require it) gave no change in the width beyond the line-fitting confidence limits.

[15]That is, the variation in fitted parameters necessary to include 67% of the experimental data. We use 101 points per line fit.

[16]C. C. Kiess and C. H. Corliss, J. Res. Natl. Bur. Stand. (U. S.) A 63, 1 (1959). These measurements were carried out at fields high enough that $\vec{I}$ and $\vec{J}$ are uncoupled.

[17]For a discussion of these, see D. M. Cox and S. J. Smith, Phys. Rev. A 5, 2428 (1972).

[18]In their recent instruction manual, NRC lists calibration factors taken from a study by R. L. Summers on hot filament ionization gauges [NASA Technical Note TN D-5285, 1969 (unpublished)]. Summers has pointed out (private communication) that these results were not intended for application to the Alphatron gauge, and that more applicable calibrations may be found in the earlier Alphatron manual and in J. R. Downing and G. Mellen, Rev. Sci. Instrum. 17, 218 (1946). We also list in Table I sensitivities relative to air from our results and from the older NRC manual. These suggest the advisability of individual calibration of these gauges.

[19]F. J. Norton, J. Am. Ceram. Soc. 36, 90 (1953).

[20]A. C. G. Mitchell and M. W. Zemansky, *Resonance Radiation and Excited Atoms* (Cambridge U. P., Cambridge, 1934).

[21]The actual situation is even more complicated due to the likelihood that there exists some absorption of the 1830-Å line within the lamp itself, due to both iodine atoms and I_2 molecules.

[22]Again, using the same hyperfine-structure correction factor of 5, as discussed by Tellinghuisen [Ref. 3(a)].

[23]We may use our result and Lawrence's ζ to calculate $\tau_r(^2P_{3/2}) = 3.2 \pm 0.5$ nsec, with all the uncertainty arising from that in ζ.

[24]E. B. Saloman and W. Happer, Phys. Rev. 144, 7 (1966).

[25]J. P. Barrat, J. Phys. Radium 20, 541 (1959); 20, 633 (1959); 20, 657 (1959).

[26]F. London, Trans. Faraday Soc. 33, 8 (1937).

[27]C. E. Moore, *Atomic Energy Levels*, NBS Circ. No. 467 (U. S. GPO, Washington, 1949, 1952, 1958).

[28]A. Dalgarno and A. E. Kingston, Proc. Roy. Soc. (London) A259, 424 (1961).

[29]J. P. Faroux and J. Brossel, Comp. Rend. 261, 3092 (1965).

[30]G. Piketty-Rives, F. Grossetete, and J. Brossel, Comp. Rend. 258, 1159 (1964).

[31]C. G. Carrington and A. Corney, J. Phys. B 4, 849 (1971).

[32]J. P. Barrat, D. Casalta, J. L. Cojan, and J. Hamel, J. Phys. (Paris) 27, 608 (1966); R. A. Phaneuf, J. Pitre, K. Hammond, and L. Krause, Can. J. Phys. 51, 724 (1973).

[33]In the original paper on this topic, Byron and Foley (Ref. 5) obtain a prediction for σ_{He}/σ_{Ne} of 0.78. This is calculated by using, for the value of $\langle pg^2 \rangle = e^2 a_0^2 \langle r^2 \rangle$, results from Slater orbitals for one electron only. If one recalculates cross sections in their formulation using Slater orbital expectation values (Ref. 34) but summing over all outer-shell electrons, the ratio becomes 0.43. Carrington and Corney (Ref. 8) predict a ratio of 0.49; the difference between their value and ours of 0.576 is due to their choice of $\langle p_i^2 \rangle$ and ΔE_1.

[34]In fact, if one excludes the $2p_2$, $2p_6$, and $2p_9$ levels as being affected by inelastic collisions and/or the repulsive part of the potential, the neon state with lowest polarizability ($12e^2a_0^2$) has the smallest ratio (0.72) and the state of highest polarizability ($71e^2a_0^2$) has the largest ratio (0.98).

[35]J. C. Slater, Phys. Rev. 36, 57 (1930).

[36]As noted by Byron and Foley (Ref. 5) these are not additive but rather the mechanism having larger of the two cross sections dominates the entire broadening process.

[37]G. Breit, Rev. Mod. Phys. 5, 91 (1933); P. Franken, Phys. Rev. 121, 508 (1961).

[38]E. U. Condon and G. H. Shortley, *The Theory of Atomic Spectra* (Cambridge U.P., Cambridge, 1963).